

Sharp enhancement on thermoelectric figure-of-merit of post-transition metal chalcogenides (PTMCs) using heterostructures with Mexican-hat valence band

Marcel S. Claro^{*1,2}

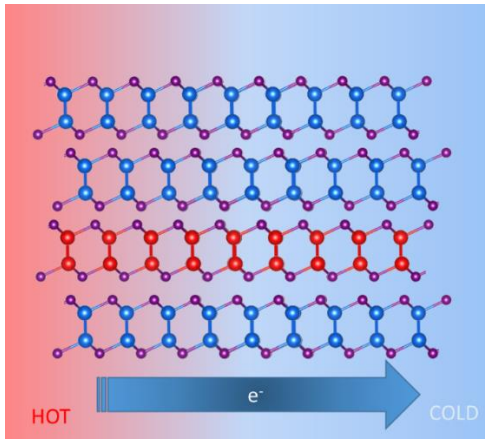
¹ INL-International Iberian Nanotechnology Laboratory, Av. Mestre José Veiga s/n, 4715-330 Braga, Portugal.

² Centro Singular de Investigación en Química Biolóxica e Materiais Moleculares (CiQUS), Departamento de Química-Física, Universidade de Santiago de Compostela, Santiago de Compostela 15782, Spain

e-mail: marcel.santos@usc.es

ABSTRACT: Post-transition metal chalcogenides (PTMCs) such as GaSe, GaS, InSe, and InS have been proposed as promising thermoelectric materials due to low lattice conductivity, originating from the atomically layered structure, high Seebeck coefficient, and the anticipation that its figure-of-merit be improved when thinned to few-layers as the band structure turns into Mexican-hat valence band (MHVB). Here we show by *ab initio* calculations that the MHVB should be present even on thick films of InSe/GaSe type-II heterostructures, and a 50% enhancement on thermoelectric figure-of-merit zT at room-temperature is expected when compared with bulk InSe.

has been proved challenging over the years, as it requires simultaneously a high Seebeck coefficient and electrical conductivity but low thermal conductivity, when high electrical conductivity actually has a detrimental effect on the electron thermal conductivity (Wiedemann-Franz law). Various methods are proposed to enhance the TE efficiency, including band engineering to improve the power factor ($S^2\sigma$), for example, using low dimensional semiconductors to obtain step-like and delta-like density of states (DOS).⁴ Another typical example is use materials with Mexican-hat valence band (MHVB), present in the most efficient TE materials, e.g., Bi_2Se_3 and Bi_2Te_3 .^{5,6} This band profile combines the large DOS and large transport velocity due to the flatness of the band. Therefore, enhancing at the same time all the TE properties.



Thermoelectric (TE) materials and devices can directly convert heat to electricity based on the Seebeck effect, and are key enabling technologies of new clean (carbon-free) sources of energy and to harvest energy which is usually wasted on inefficient equipment and energy generation.¹⁻³ Nonetheless, The main obstacle to the wide adoption of TE devices is their low efficiency. The efficiency of thermoelectric materials is measured by the figure-of-merit $zT(T) = S^2\sigma T / (\kappa_e + \kappa_L)$, where S is the Seebeck coefficient, σ is the electrical conductivity, T is the absolute temperature, κ_L and κ_e are the lattice and electronic thermal conductivities, respectively. Increase zT value

Mexican-hat dispersions are relatively common in few-layer two-dimensional materials. *Ab initio* studies and ARPES direct measurements have found Mexican-hat dispersions in the valence band of many few-layer Post-transition metal chalcogenides (PTMCs) materials such as GaSe, GaS, InSe, and InS.⁷⁻⁹ These materials are interesting for electronic and photonic application and also have been proposed as promising TE due to their low lattice conductivity ($< 2 \text{ W m}^{-1} \text{ K}^{-1}$)¹⁰, high Seebeck coefficient¹¹, and the anticipation that its figures-of-merit be improved when thinned to TL scale, due to the increment of the density of states (DOS) when the band structure turns into MHVB.^{5,6} Such thin PTMCs in theory would present zT as high as 2.05 and as good as the reference Bi_2Te_3 alloys. Nevertheless, the MHVB only appears in those materials in the form of very thin films, with less than 7 TLs¹² which results in difficulties to practical exploit its properties, including the growth or transfer of such thin films, the stability of the material in air^{13,14}, and the difficulties to measure tiny signals and properties at (Se-Ga(In)-Ga(In)-Se) tetralayer (TL) scale. For these reasons, despite the early theoretical interest, there are not experimental reports to date on the thermoelectric properties of few-layers PTMCs. Here we show that short-period GaSe/InSe superlattices (SL) share the same valence band properties. As a result, important electronic properties, in particular the thermoelectric figures-of-merit, that have already been calculated or measured in samples of few-layer thickness would be comparable in superlattices with the advantage of been amplified by

the film thickness (number of SL periods) and facilitated application.

Starting from the indication that the MHVB is stronger in thinner films.^{5,12} We performed calculations based on plane-waves density functional theory (DFT) to obtain the band structure of several InSe/GaSe SLs containing 1 to 3 TLs of GaSe in a 4 TL SL unit cell (Table 1). In this case, InSe replaces the vacuum of isolated layers as a barrier, due to type-II band alignments. In comparison to isolated layers, similar valley depth and peak k-point is obtained⁵. The SL with deepest valley (3 TL InSe / 1 TL GaSe SL) is then used in the following calculations.

Table 1. Comparison Γ -valley depth and peak k-point of the top of valence band for 4 TL SL unit cell heterostructures with ϵ -($\bar{P}6m2$) stack using PBEsol functional.

	Γ -valley depth (meV)	Peak k-point (\AA^{-1})
1 TL GaSe/3 TL InSe	54	0.132
2 TL GaSe/2 TL InSe	45	0.118
3 TL GaSe/1 TL InSe	21	0.096

GaSe and InSe have several known polymorphs appearing depending on the growth method, the most common polytypes with non-centrosymmetric TL (D_{3h}) are named as ϵ -($\bar{P}6m2$), β -($P6_3/mmc$), γ -($R3m$), and δ -($P6_3mc$), based on different stacking sequences between the adjacent layers.^{15–18} Nevertheless, we reported recently the first structural observation of a new GaSe and InSe polymorph ($R\bar{3}m$) (named as γ' -polymorph) characterized by a distinct atomic configuration with centrosymmetric TL (D_{3d}).^{17,19,20} When with the same monolayer symmetry, polymorphs present small differences in band structure, electronic and optical properties particularities due to the presence or lack of special symmetries, however, usually these differences are not noticeable in most practical uses. Considering it, despite the γ' and γ are the most common polytypes in our SL growth by MBE, we use the ϵ -stack and its centrosymmetric version $P6_3/mc$ (named as ϵ' -polymorph) to compare between the D_{3h} and D_{3d} TLs SL, and these results should extend to the same TL symmetry polytypes. It is convenient not just because of the smaller unit cell (2 vs 3 TL) but also because the γ is rhombohedral with a different k-space, with A-A bandgap instead of Γ - Γ .¹⁶ In the Figure 1 we show the comparison between D_{3h} and D_{3d} TLs SL band structure using Perdew-Burke-Ernzerhof (PBEsol)²¹ generalized-gradient-approximation (GGA). We observe a small difference in the bandgap in the Γ - and M-point, a larger bandgap difference, and a spin degeneracy break in the K-point (D_{3d} full Brillouin path in the supplementary information), however, more importantly, is the shape of the valence band. The centrosymmetric TL SL is the only one having MHVB. It suggests that the electronic hybridization between the TLs is reduced in the D_{3d} polymorphs²² and makes it a case closer to isolated TL.

Since the PBEsol functional is well-known to underestimate the bandgap, in the following calculations we used the modified Becke-Johnson exchange-correlation (mBJ) potential²³, which provides more accurate bandgaps and band structures in comparison to many-body theory (G_0W_0) and experimental data after the calibration of the *parameter c* that weights the

Becke-Russel exchange¹⁶. In this way is not necessary to deal with scissor operators when the properties depend on the bandgap, as the properties of interest. For GaSe and InSe the *parameter c* was fixed ($c = 0.838$) after obtain the experimental band gap of β -InSe(D_{3h} TL) (1.25^{15,16} eV). In the mBJ calculations (Figure 2a) the Γ -valley shows a depth of 17 meV and radius of 0.094 \AA^{-1} . These are the main MHVB features, from which most of the characteristic material properties derive, and they are similar to the values found experimentally in isolated 2 TL GaSe⁷. The comparison between the functionals (Figure 2a), shows that these values can change slightly depending on the chosen functional, but the MHVB shape largely remains unaltered.

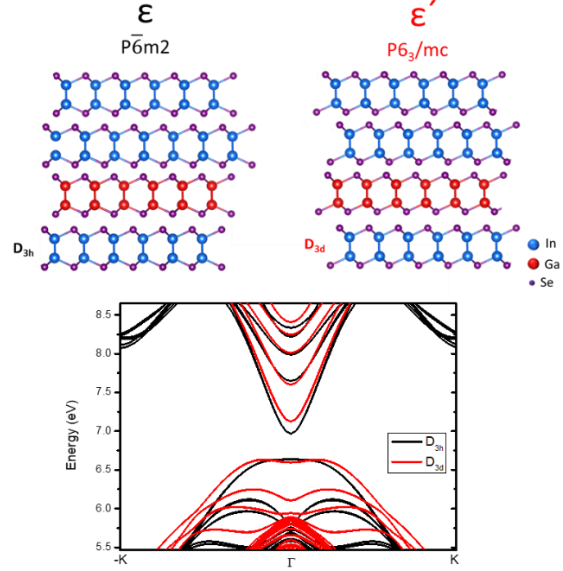


Figure 1. Comparison of crystal structure (top) of 1 TL GaSe/ 3 TL InSe with centrosymmetric (D_{3d}) and non-centrosymmetric (D_{3h}) TLs in a ϵ -type stack along the $[10\bar{1}0]$ plane, and its band structures around the Γ -point (bottom).

We proceed with our analysis taking InSe as a reference since this SL is actually $\frac{3}{4}$ InSe. Figure 2b makes this comparison with the calculated DOS. While the conduction band DOS is very similar on both materials, the SL exhibits van Hove singularities in the region where InSe has the standard parabolic band DOS due to MHVB. To state how it reflects in the TE properties, we performed a estimation of S , the power-factor ($S^2\sigma$), and zT (Figure 3) which is straightforward from the band structure and DOS, making use of Boltzmann equation²⁴. The Seebeck coefficient, conductivity (σ/τ) and electronic thermal conductivity (k_e/τ) are calculated using BoltzTraP package and the output of DFT-mBJ. τ is the electron scattering time. The unknown values (τ and κ_L) can be obtained experimentally or from first principles calculations. In this work, τ (derivated from mean free path $\lambda_0=25$ nm) is extracted the literature²⁵ based on conductivity experimental data. The κ_L (T) is obtained from first-principles calculations and is also in agreement with experimental values.²⁶ In fact, the zT and Seebeck coefficient obtained for bulk InSe are similar to experimental data^{11,27} which validates these approximations.

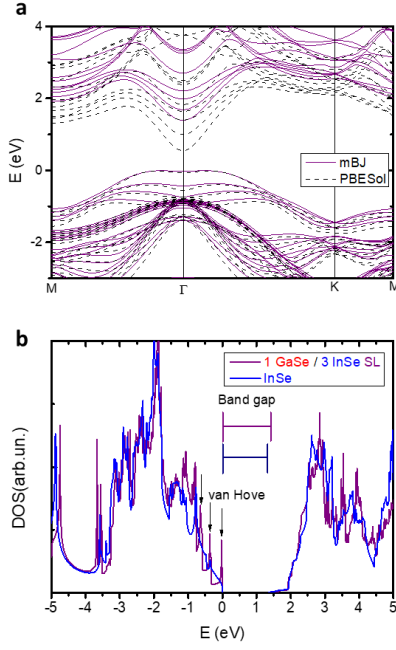


Figure 2. a) Calculated band structure of ϵ' -polymorph bulk 3 InSe TL / 1 GaSe TL superlattice (3/1 TL SL) using mBJ and PBEsol functional b) Density of states (DOS) of ϵ' -polymorph bulk InSe and 1 TL GaSe / 3 TL InSe SL.

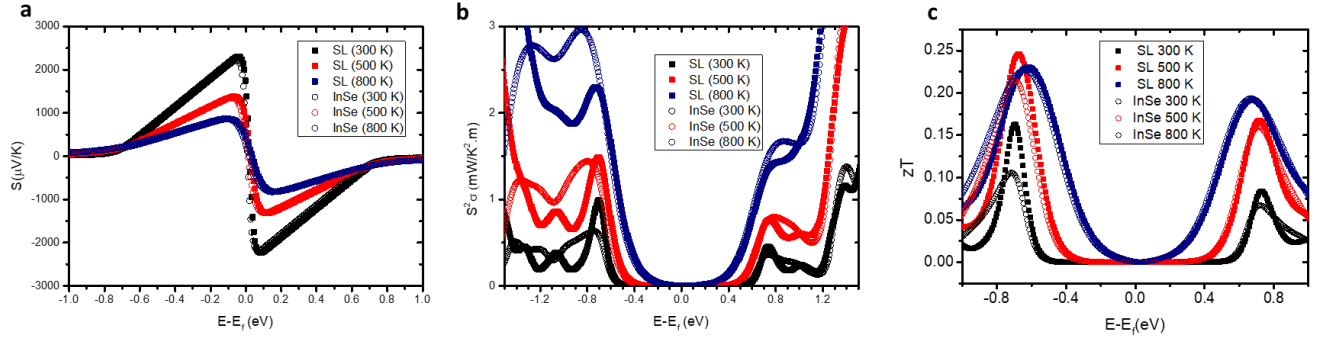


Figure 3. a) Seebeck coefficient, b) power factor c) zT thermoelectric figure-of-merit of InSe and 3/1 TL SL in function of temperature and chemical potential between 300 and 800 K.

In conclusion, using *ab initio* calculations we demonstrate that the in-plane zT can increase about 50% at room temperature in p-type on GaSe/InSe superlattices in comparison to bulk InSe due to the singularities in the DOS, which are present in the Mexican-hat valence band. MHVB exists only on non-centrosymmetric TL(D_{3d}) SL, and a 1 TL GaSe / 3 TL InSe SL presents a valence band shape which is similar to an isolated 2 TL GaSe. Similarly, this concept can be applied in other PTMCs, which are already considered as promising multifunctional materials, to enhance its performance as thermoelectric materials.

Method

The *ab initio* calculations were done using density perturbation theory (DFT) within the Perdew-Burke-Ernzerhof

Our calculations show that in comparison to bulk InSe the Seebeck coefficient barely changes for all temperatures and chemical potential considered. However, the singularities in the DOS caused by the MHVB result in a considerable increase in the electrical conductivity and the power factor without a corresponding increase in the κ_e . The outcome is that in-plane zT sharp increases (about 50%) at room temperature in p-type SL. There is also a reduction of 200 K in the optimum temperature which makes it even more attractive for several applications at room-temperature. This increment in zT can be even bigger considering the improvement in κ_L that occurs in SLs due to phonon confinement²⁸ in the heterostructure interfaces, and that was not considered in this first approximation.

We recently presented the epitaxial growth of InSe/GaSe heterostructures with atomically defined interfaces and D_{3d} polymorphs using molecular beam epitaxy (MBE), which makes these superlattices readily available.²⁰ Few candidates for doping of PTMC already exist and can be used to achieve the chemical potential for peak zT .^{29–32} While MBE would be a method appropriate for high-value wafers, other methods like chemical vapor deposition³³ (CVD), pulsed-laser deposition³⁴ (PLD) can be used to produce inexpensive large surfaces of this material in the future. Yet, The van der Waals (vdW) bond between the PTMC layers and the substrate facilitates the growth on a great variety of substrates and surface.

(PBEsol)²¹ generalized-gradient-approximation (GGA) and the modified Becke-Johnson exchange-correlation (mBJ meta-GGA) as implemented in Quantum Espresso^{35,36} (QE) and LIBXC³⁷ using norm-conserving pseudopotentials³⁸. We have optimized lattice parameters and atomic positions using PBEsol until forces in each atom are smaller than 0.01 eV/Å. For all systems, the basis-set cutoff energy is 140 Ry and the Brillouin zone integrated with 15x15x6 Γ -centered Monkhorst-Pack grid of k-points for bulk materials (β - ϵ -polytypes) and 15x15x3 grids for the 2 unit cells superlattices in the self-consistent calculations with convergence criteria of 1×10^{-8} eV. We used twice the number of points (31x31x10 and 31x31x6) in non-self-consistent calculations for DOS and transport properties using BoltzTraP²⁴, which interpolate each k-point with 5 more intermediary points.

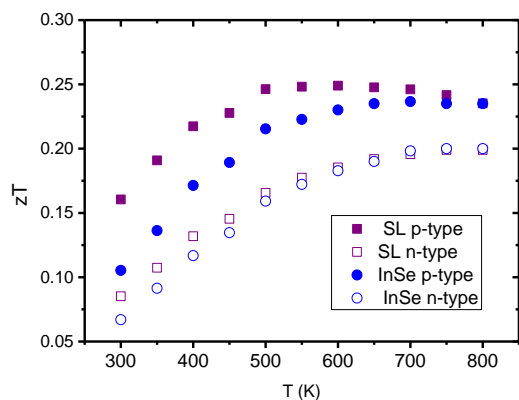


Figure 4. Comparison of Peak in-plane zT of n- and p-type bulk InSe and 1 TL GaSe/ 3 TL InSe SL between 300 K and 800 K.

ACKNOWLEDGMENT

The computations were performed on the Tirant III cluster of the Servei d'Informàtica of the University of Valencia (project vlc82) thanks to Alejandro Molina-Sánchez and the Darwin cluster of INL-International Iberian Nanotechnology Laboratory thanks to Joaquín F. Rossier.

REFERENCES

- (1) Bell, L. E. Cooling, Heating, Generating Power, and Recovering Waste Heat with Thermoelectric Systems. *Science*. American Association for the Advancement of Science September 12, 2008, pp 1457–1461. <https://doi.org/10.1126/science.1158899>.
- (2) Zhang, X.; Zhao, L. D. Thermoelectric Materials: Energy Conversion between Heat and Electricity. *Journal of Materiomics*. Chinese Ceramic Society June 1, 2015, pp 92–105. <https://doi.org/10.1016/j.jmat.2015.01.001>.
- (3) Petsagkourakis, I.; Tybrandt, K.; Crispin, X.; Ohkubo, I.; Satoh, N.; Mori, T. Thermoelectric Materials and Applications for Energy Harvesting Power Generation. *Sci. Technol. Adv. Mater.* **2018**, *19* (1), 836–862. <https://doi.org/10.1080/14686996.2018.1530938>.
- (4) Hicks, L. D.; Dresselhaus, M. S. Effect of Quantum-Well Structures on the Thermoelectric Figure of Merit. *Phys. Rev. B* **1993**, *47* (19), 12727–12731. <https://doi.org/10.1103/PhysRevB.47.12727>.
- (5) Wickramaratne, D.; Zahid, F.; Lake, R. K. Electronic and Thermoelectric Properties of van Der Waals Materials with Ring-Shaped Valence Bands. *J. Appl. Phys.* **2015**, *118* (7), 075101. <https://doi.org/10.1063/1.4928559>.
- (6) Nurhuda, M.; Nugraha, A. R. T.; Hanna, M. Y.; Suprayoga, E.; Hasdeo, E. H. Thermoelectric Properties of Mexican-Hat Band Structures. *Adv. Nat. Sci. Nanosci. Nanotechnol.* **2020**, *11* (1), 015012. <https://doi.org/10.1088/2043-6254/ab7225>.
- (7) Chen, M.-W.; Kim, H.; Ovchinnikov, D.; Kuc, A.; Heine, T.; Renault, O.; Kis, A. Large-Grain MBE-Grown GaSe on GaAs with a Mexican Hat-like Valence Band Dispersion. *npj 2D Mater. Appl.* **2018**, *2* (1), 2. <https://doi.org/10.1038/s41699-017-0047-x>.
- (8) Hamer, M. J.; Zultak, J.; Tyurnina, A. V.; Zólyomi, V.; Terry, D.; Barinov, A.; Garner, A.; Donoghue, J.; Rooney, A. P.; Kandyba, V.; Giampietri, A.; Graham, A.; Teutsch, N.; Xia, X.; Koperski, M.; Haigh, S. J.; Fal'ko, V. I.; Gorbachev, R. V.; Wilson, N. R. Indirect to Direct Gap Crossover in Two-Dimensional InSe Revealed by Angle-Resolved Photoemission Spectroscopy. *ACS Nano* **2019**, *13* (2), 2136–2142. <https://doi.org/10.1021/acsnano.8bo8726>.

- (9) Shevitski, B.; Ulstrup, S.; Koch, R. J.; Cai, H.; Tongay, S.; Moreschini, L.; Jozwiak, C.; Bostwick, A.; Zettl, A.; Rotenberg, E.; Aloni, S. Tunable Electronic Structure in Gallium Chalcogenide van Der Waals Compounds. *Phys. Rev. B* **2019**, *100* (16), 165112. <https://doi.org/10.1103/PhysRevB.100.165112>.
- (10) Liu, Y.; Wang, W.; Yang, J.; Li, S. Recent Advances of Layered Thermoelectric Materials. *Adv. Sustain. Syst.* **2018**, *2* (8–9), 1800046. <https://doi.org/10.1002/adsu.201800046>.
- (11) Han, G.; Chen, Z.-G.; Drennan, J.; Zou, J. Indium Selenides: Structural Characteristics, Synthesis and Their Thermoelectric Performances. *Small* **2014**, *10* (14), 2747–2765. <https://doi.org/10.1002/smll.201400104>.
- (12) Hamer, M. J.; Zultak, J.; Tyurnina, A. V.; Zólyomi, V.; Terry, D.; Barinov, A.; Garner, A.; Donoghue, J.; Rooney, A. P.; Kandyba, V.; Giampietri, A.; Graham, A.; Teutsch, N.; Xia, X.; Koperski, M.; Haigh, S. J.; Fal'ko, V. I.; Gorbachev, R. V.; Wilson, N. R. Indirect to Direct Gap Crossover in Two-Dimensional InSe Revealed by Angle-Resolved Photoemission Spectroscopy. *ACS Nano* **2019**, *13* (2), 2136–2142. <https://doi.org/10.1021/acsnano.8bo8726>.
- (13) Beechem, T. E.; Kowalski, B. M.; Brumbach, M. T.; McDonald, A. E.; Spataru, C. D.; Howell, S. W.; Ohta, T.; Pask, J. A.; Kalugin, N. G. Oxidation of Ultrathin GaSe. *Appl. Phys. Lett.* **2015**, *107* (17), 173103. <https://doi.org/10.1063/1.4934592>.
- (14) Kowalski, B. M.; Manz, N.; Bethke, D.; Shaner, E. A.; Serov, A.; Kalugin, N. G. Role of Humidity in Oxidation of Ultrathin GaSe. *Mater. Res. Express* **2019**, *6* (8), 085907. <https://doi.org/10.1088/2053-1591/ab1dd2>.
- (15) Magorrian, S. J.; Zólyomi, V.; Drummond, N. D. Structures of Bulk Hexagonal Post Transition Metal Chalcogenides from Dispersion-Corrected Density Functional Theory. *Phys. Rev. B* **2021**, *103* (9), 094118. <https://doi.org/10.1103/PhysRevB.103.094118>.
- (16) Srour, J.; Badawi, M.; El Haj Hassan, F.; Postnikov, A. Comparative Study of Structural and Electronic Properties of GaSe and InSe Polytypes. *J. Chem. Phys.* **2018**, *149* (5), 054106. <https://doi.org/10.1063/1.5030539>.
- (17) Sun, Y.; Li, Y.; Li, T.; Biswas, K.; Patané, A.; Zhang, L. New Polymorphs of 2D Indium Selenide with Enhanced Electronic Properties. *Adv. Funct. Mater.* **2020**, *2001920*. <https://doi.org/10.1002/adfm.202001920>.
- (18) Bergeron, H.; Lebedev, D.; Hersam, M. C. Polymorphism in Post-Dichalcogenide Two-Dimensional Materials. *Chemical Reviews*. American Chemical Society February 24, 2021, pp 2713–2775. <https://doi.org/10.1021/acs.chemrev.0c00933>.
- (19) Nitta, H.; Yonezawa, T.; Fleurence, A.; Yamada-Takamura, Y.; Ozaki, T. First-Principles Study on the Stability and Electronic Structure of Monolayer GaSe with Trigonal-Antiprismatic Structure. *Phys. Rev. B* **2020**, *102* (23), 235407. <https://doi.org/10.1103/PhysRevB.102.235407>.
- (20) Claro, M. S.; Martínez-Pastor, J. P.; Molina-Sánchez, A.; Hajraoui, K. El; Grzonka, J.; Adl, H. P.; Marrón, D. F.; Ferreira, P. J.; Bondarchuk, A.; Sadewasser, S. The Quantum-Well Turn into van Der Waals: Epitaxy of GaSe and InSe Heterostructures for Optoelectronic Devices. **2022**.
- (21) Csonka, G. I.; Perdew, J. P.; Ruzsinszky, A.; Philipson, P. H. T.; Lebègue, S.; Paier, J.; Vydrov, O. A.; Ángyán, J. G. Assessing the Performance of Recent Density Functionals for Bulk Solids. *Phys. Rev. B - Condens. Matter Mater. Phys.* **2009**, *79* (15), 155107. <https://doi.org/10.1103/PhysRevB.79.155107>.
- (22) Zribi, J.; Khalil, L.; Zheng, B.; Avila, J.; Pierucci, D.; Brulé, T.; Chaste, J.; Lhuillier, E.; Asensio, M. C.; Pan, A.; Querghi, A. Strong Interlayer Hybridization in the Aligned SnS₂/WSe₂ Hetero-Bilayer Structure. *npj 2D Mater. Appl.* **2019**, *3* (1), 27. <https://doi.org/10.1038/s41699-019-0109-3>.
- (23) Tran, F.; Blaha, P. Accurate Band Gaps of Semiconductors and Insulators with a Semilocal Exchange-Correlation

- Potential. *Phys. Rev. Lett.* **2009**, *102* (22), 226401. <https://doi.org/10.1103/PhysRevLett.102.226401>.
- (24) Madsen, G. K. H.; Singh, D. J. BoltzTraP. A Code for Calculating Band-Structure Dependent Quantities. *Comput. Phys. Commun.* **2006**, *175* (1), 67–71. <https://doi.org/10.1016/j.cpc.2006.03.007>.
- (25) Wickramaratne, D.; Zahid, F.; Lake, R. K. Electronic and Thermoelectric Properties of van Der Waals Materials with Ring-Shaped Valence Bands. *J. Appl. Phys.* **2015**, *118* (7), 075101. <https://doi.org/10.1063/1.4928559>.
- (26) Haleoot, R.; Hamad, B. Thermoelectric Properties of Doped β -InSe by Bi: First Principle Calculations. *Phys. B Condens. Matter* **2020**, *587*, 412105. <https://doi.org/10.1016/j.physb.2020.412105>.
- (27) Lee, K. H.; Oh, M.-W.; Kim, H.-S.; Shin, W. H.; Lee, K.; Lim, J.-H.; Kim, J.; Kim, S. Enhanced Thermoelectric Transport Properties of N-Type InSe Due to the Emergence of the Flat Band by Si Doping. *Inorg. Chem. Front.* **2019**, *6* (6), 1475–1481. <https://doi.org/10.1039/C9QI100210C>.
- (28) Venkatasubramanian, R. Lattice Thermal Conductivity Reduction and Phonon Localizationlike Behavior in Superlattice Structures. *Phys. Rev. B - Condens. Matter Mater. Phys.* **2000**, *61* (4), 3091–3097. <https://doi.org/10.1103/PhysRevB.61.3091>.
- (29) Micocci, G.; Molendini, M.; Tepore, A.; Rella, R.; Siciliano, P. Investigation of the Electrical Properties of Cd-Doped Indium Selenide. *J. Appl. Phys.* **1991**, *70* (11), 6847–6853. <https://doi.org/10.1063/1.349807>.
- (30) Shigetomi, S.; Ikari, T.; Nishimura, H. Photoluminescence Spectra of P-GaSe Doped with Cd. *J. Appl. Phys.* **1991**, *69* (11), 7936–7938. <https://doi.org/10.1063/1.347488>.
- (31) Micocci, G.; Serra, A.; Tepore, A. Electrical Properties of N-GaSe Single Crystals Doped with Chlorine. *J. Appl. Phys.* **1997**, *82* (5), 2365–2369. <https://doi.org/10.1063/1.366046>.
- (32) Segura, A.; Martínez-Tomás, M. C.; Marí, B.; Casanovas, A.; Chevy, A. Acceptor Levels in Indium Selenide. An Investigation by Means of the Hall Effect, Deep-Level-Transient Spectroscopy and Photoluminescence. *Appl. Phys. A Solids Surfaces* **1987**, *44* (3), 249–260. <https://doi.org/10.1007/BF00616698>.
- (33) Balakrishnan, N.; Steer, E. D.; Smith, E. F.; Kudrynskiy, Z. R.; Kovalyuk, Z. D.; Eaves, L.; Patané, A.; Beton, P. H. Epitaxial Growth of γ -InSe and α , β , and γ -In₂Se₃ on ϵ -GaSe. *2D Mater.* **2018**, *5* (3), 035026. <https://doi.org/10.1088/2053-1583/aac479>.
- (34) Bergeron, H.; Guiney, L. M.; Beck, M. E.; Zhang, C.; Sangwan, V. K.; Torres-Castaneda, C. G.; Gish, J. T.; Rao, R.; Austin, D. R.; Guo, S.; Lam, D.; Su, K.; Brown, P. T.; Glavin, N. R.; Maruyama, B.; Bedzyk, M. J.; Dravid, V. P.; Hersam, M. C. Large-Area Optoelectronic-Grade InSe Thin Films via Controlled Phase Evolution. *Appl. Phys. Rev.* **2020**, *7* (4), 041402. <https://doi.org/10.1063/5.0023080>.
- (35) Giannozzi, P.; Andreussi, O.; Brumme, T.; Bunau, O.; Buongiorno Nardelli, M.; Calandra, M.; Car, R.; Cavazzoni, C.; Ceresoli, D.; Cococcioni, M.; Colonna, N.; Carnimeo, I.; Dal Corso, A.; De Gironcoli, S.; Delugas, P.; Distasio, R. A.; Ferretti, A.; Floris, A.; Fratesi, G.; Fugallo, G.; Gebauer, R.; Gerstmann, U.; Giustino, F.; Gorni, T.; Jia, J.; Kawamura, M.; Ko, H. Y.; Kokalj, A.; Küçükbenli, E.; Lazzeri, M.; Marsili, M.; Marzari, N.; Mauri, F.; Nguyen, N. L.; Nguyen, H. V.; Otero-De-La-Roza, A.; Paulatto, L.; Poncé, S.; Rocca, D.; Sabatini, R.; Santra, B.; Schlipf, M.; Seitsonen, A. P.; Smogunov, A.; Timrov, I.; Thonhauser, T.; Umari, P.; Vast, N.; Wu, X.; Baroni, S. Advanced Capabilities for Materials Modelling with Quantum ESPRESSO. *J. Phys. Condens. Matter* **2017**, *29* (46), 465901. <https://doi.org/10.1088/1361-648X/aa8f79>.
- (36) Giannozzi, P.; Baroni, S.; Bonini, N.; Calandra, M.; Car, R.; Cavazzoni, C.; Ceresoli, D.; Chiarotti, G. L.; Cococcioni, M.; Dabo, I.; Dal Corso, A.; De Gironcoli, S.; Fabris, S.; Fratesi, G.; Gebauer, R.; Gerstmann, U.; Gougoussis, C.; Kokalj, A.; Lazzeri, M.; Martin-Samos, L.; Marzari, N.; Mauri, F.; Mazzarello, R.; Paolini, S.; Pasquarello, A.; Paulatto, L.; Sbraccia, C.; Scandolo, S.; Sclauzero, G.; Seitsonen, A. P.; Smogunov, A.; Umari, P.; Wentzcovitch, R. M. QUANTUM ESPRESSO: A Modular and Open-Source Software Project for Quantum Simulations of Materials. *J. Phys. Condens. Matter* **2009**, *21* (39), 395502. <https://doi.org/10.1088/0953-8984/21/39/395502>.
- (37) Lehtola, S.; Steigemann, C.; Oliveira, M. J. T.; Marques, M. A. L. Recent Developments in LIBXC — A Comprehensive Library of Functionals for Density Functional Theory. *SoftwareX* **2018**, *7*, 1–5. <https://doi.org/10.1016/j.softx.2017.11.002>.
- (38) Hamann, D. R. Optimized Norm-Conserving Vanderbilt Pseudopotentials. *Phys. Rev. B - Condens. Matter Mater. Phys.* **2013**, *88* (8), 085117. <https://doi.org/10.1103/PhysRevB.88.085117>.

Supplementary Information

Sharp enhancement on thermoelectric figure-of-merit of post-transition metal chalcogenides (PTMCs) using heterostructures with Mexican-hat valence band

Marcel S. Claro^{*1,2}

¹ INL-International Iberian Nanotechnology Laboratory, Av. Mestre José Veiga s/n, 4715-330 Braga, Portugal.

² Centro Singular de Investigación en Química Biolóxica e Materiais Moleculares (CiQUS), Departamento de Química-Física, Universidade de Santiago de Compostela, Santiago de Compostela 15782, Spain

e-mail: marcel.santos@usc.es

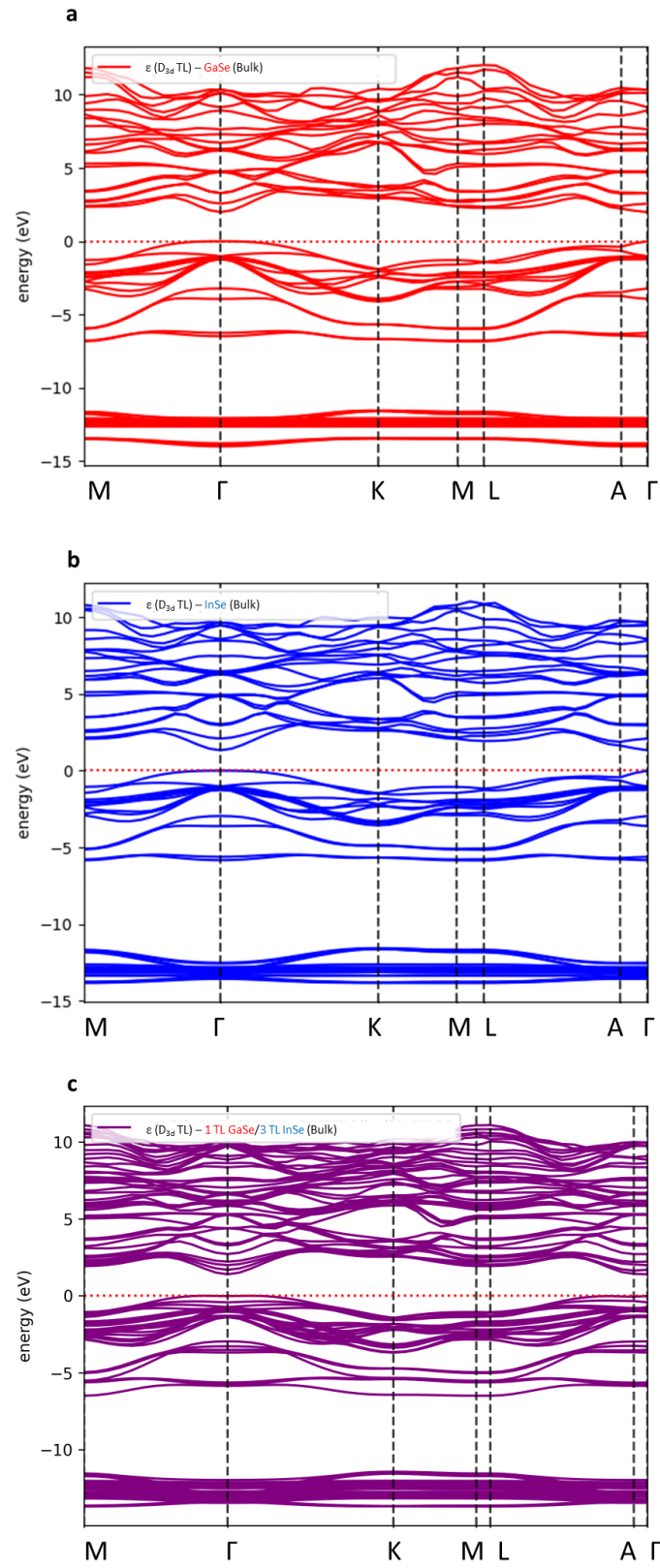


Figure S1. Band structure of $P6_3/mc$ polytype of GaSe (a), InSe (b) and superlattice (c).